

# Splitting Forces in FRPR Pretensioned Concrete

by W.R. de Sitter and R.A. Vonk

Synopsis: In concrete pretensioned with non-metallic Fiber Reinforced Plastic Reinforcement (FRPR) the Hoyer effect leads to high splitting stresses due to confinement of radial deformations of bars or strands in the transfer zone. Incompatible linear temperature expansion can aggravate the splitting stresses. Bond in the transfer zone is heavily influenced by the confined radial expansion as demonstrated by tests with Arapree bars in light weight concrete. Very short transfer lengths (80 mm) have been measured. Three calculation approaches for splitting stresses are presented; the Elasto Plastic approach, the Concrete Deformation approach and the Fracture Energy approach. The Elasto Plastic model has been checked using a discrete element model including tensile softening of concrete. The presented formula are confirmed by a few tests on Arapree pretensioned prisms.

Keywords: Fiber reinforced plastics; lightweight concrete; pretensioning; splitting stresses; stress transfer

## 2 de Sitter and Vonk

W. Reinold de Sitter  
Hollandsche Beton Groep nv director R&D  
Eindhoven University of Technology  
parttime professor for Concrete Structures with the  
Faculty of Architecture and Building Science

René A. Vonk  
Eindhoven University of Technology  
Completed his PhD-thesis on softening of concrete and  
received his doctor's title in 1992 at the  
Faculty of Architecture and Building Science

### INTRODUCTION

The transfer of prestress in pretensioned concrete leads to tensile splitting stresses in the anchorage zone. These can be attributed to two causes (fig. 1).

1. The Hoyer effect; release of pretension causes radial expansion of the prestress material due to its Poisson coefficient. This leads to radial compressive stresses resulting in increased bond in the anchorage zone.

2. Transfer of bond stresses along a prestress bar or strand in the anchorage zone introduces tensile stresses in the tangential direction in the concrete.

The Hoyer effect is restrained by the concrete leading to radial stresses  $p_r$  normal to the interface of the bar/strand with the concrete. A high level of  $p_r$  increases the bond stresses and the angle  $\phi$ . Therefore both causes of splitting forces are interrelated. In section 3 it will be shown that even in the case of smooth surface texture and very low bond the Hoyer effect may lead to splitting. At the extreme end of the anchorage zone the shear stress  $\tau_{tr}$  must be zero because  $\tau_{r1}$  is zero at the free concrete surface. In this area the Hoyer effect will dominate the splitting forces. The material properties make FRPR sensitive to the Hoyer effect.

The coefficient of radial thermal expansion  $\alpha_r$  of FRPR is governed by the (more or less) linear thermal expansion of the bonding resin. In many types of FRPR the value of  $\alpha_r$  is 5 to 8 times the value for concrete. An increase in temperature then will lead to tangential splitting stresses in the concrete. The combination of thermal stresses with stresses caused by the Hoyer effect and prestress force transfer did lead to severe longitudinal cracking in thin pretensioned elements (fig.2).

#### Acknowledgement

This research program is supported by the European Community through the Brite-Euram program.

THE HOYER EFFECT COMBINED WITH TEMPERATURE EXPANSION

The E-modulus  $E_1$  in the longitudinal direction of FRPR is governed by the E-modulus  $E_{1f}$  of the fibers. The E-moduli vary from 80 000 to 140 000 MPA for aramid fibers and 4000 to 6000 MPA for resins. If the contribution of the resin is neglected:

$$E_1 = A_f E_{1f} / A_1$$

The longitudinal strain  $\varepsilon_{1f0}$  and the radial contraction  $\varepsilon_{r0}$  in prestensioned state:

$$\varepsilon_{10} \approx \sigma_{1f0} / E_{1f} = \sigma_{10} / E_1$$

$$\varepsilon_{r0} = \nu_r \varepsilon_{10}$$

The radial contraction is governed by the poisson coefficient  $\nu_{res}$  of the resin if we neglect the influence of the radial contraction of the fibers.

After release of pretension the expansion of the resin in the longitudinal direction is restrained by the concrete and by the fibers.

Transfer zone:

$$\varepsilon_{r1} = \nu_{res} \varepsilon_{10} + (\alpha_{res} - \alpha_c) \Delta T \quad (1)$$

and

$$p_{r1} = \varepsilon_{r1} E_{res} / (1 - \nu_{res}) \quad (2)$$

After the transfer zone radial expansion due to release of pretension does not play a role but longitudinal deformation of the resin is restrained by the fibers as well as the surrounding concrete. Hence, the apparent modulus varies between  $E_{res}/(1 - \nu_{res})$  and  $E_{res}/(1 - \nu_{res} - 2\nu_{res}^2)$

After the transfer zone:

$$\varepsilon_{r1} = +(1 + \nu_{res})(\alpha_{res} - \alpha_c) \Delta T \quad (3)$$

After the transfer:

$$p_{r1} = \varepsilon_{r1} E_{res} / (1 - \nu_{res} - 2\nu_{res}^2) \quad (4)$$

These expressions may be refined to include combined moduli of fibers and resin according to volumetric laws. However even a small amount of enclosed air may have a large influence on composite moduli in the transverse direction. Therefore composite moduli must be measured on representative samples; they can only be approximated from the moduli of the constituent materials.

## 4 de Sitter and Vonk

Comparing expression (2) and (4) it follows that, depending on the relative relation between the Hoyer stress and the temperature induced stresses cracking will start either in the anchorage zone or at some distance from the free end.

### PULL-OUT AND PUSH-IN BOND STRENGTH

In pretensioned concrete bond in the transfer zone is identical with bond as observed in a push-in test. However in the ultimate load situation bond in the anchorage zone is more analogous with a pull-out condition.

The influence of transverse expansion and contraction on bond has been investigated by comparison of bond in pull-out and push-in tests (fig.3) [1]. These tests were too few to permit firm quantitative conclusions but they indicate significant differences in bond. In the push-in tests arapree bars (nominal: 8 mm) with embedded sand were tensioned to values varying between 23.64 and 26.46 kN. The circular samples of lightweight concrete were cast around these bars with cover 21 to 35 mm. After 3 days wet curing the tensile splitting strength  $f_{ct}$  was 1.6 to 2.5 MPa. Then the force  $F_1$  in the upper part of the bar was gradually released. The reaction forces were measured as a check on  $(F_2 - F_1)$  as well as the slip of the bar with respect to the l.w. concrete. In the pull-out tests the bars were stressed to a force 2.4 - 6.6 kN. Then the force  $F_2$  in the lower half of the bar was increased. The mean bond stress  $\tau$  was evaluated taking into account the embedded length of 35 mm, the actual circumference of the bar and the peak value of  $(F_2 - F_1)$ . The maximum observed values  $\tau_{max}$  averaged over 35 mm are listed in Table 1. Visible cracking and crack pattern were noted.

As expected the push-in tests showed more cracking than the pull-out tests. In series 3 (the only non cracked push-in test) the average push-in bond stress was 11.07 MPa as compared to 6.74 MPa in the case of the corresponding pull-out test.

### TRANSFER LENGTH AND SPLITTING

Transfer length and splitting were further investigated [2] in tests on 300 mm long prisms pretensioned with 5.7 mm Arapree bars at a nominal jacking force of 17 kN. Four types of surface texture were included, varying from perfectly smooth to coarse embedded sand. Prisms had sides of 30, 35, 40 and 45 mm.

In table 2 the occurrence of cracking is summarized. The 40\*40 prism showed cracks (fig. 4) after an interval varying between 1 minute to 3 months after testing. Typical strains measured at the concrete surface are given in fig. 5. The considerable spread is attributed to local differences in concrete E-modulus due to aggregate distribution.

The modulus  $E_{fr}$  of the fibers is 120 000 MPa and the cross section of 100 000 fibers in the 5.7 mm bar is 11.1 mm<sup>2</sup>.

$$\epsilon_{r10} = 17000/(11.1*120000)=1.28\%$$

$$\epsilon_{r0} = -\nu \epsilon_{r10} = -0.35*1.276\%=-0.45\%$$

$$p_{r1} = 0.0045*4000/(1-0.35) = 28\text{MPa}$$

### CALCULATIONS

Cracking due to the Hoyer effect has been simulated by Van Gils [2] using the computer program UDEC. The effect of splitting stresses in two dimensional cross-sections of square and circular prisms were investigated. Only the results for a circular cross-section are discussed here, as they differ only slightly from the results for a square cross-section and can be used for comparison with simple design formulas. Three discrete radial cracks were modelled in the simulations, since the tests almost always showed failure due to the formation of three cracks.

### Conclusions:

- a] Embedded sand in the surface is essential to transfer of pretension. However, if some sand is embedded the amount and coarseness of the sand has not a dominant influence on the transfer length, which varies between 60 and 120 mm. (In [3] a transfer length of 135 mm in the case of 20\*2,6 mm<sup>2</sup> flat Arapree strips was reported).
- b] Prisms with smooth bars show a very reduced transfer of pretension but they crack nonetheless. Thus showing the predominant influence of the Hoyer effect on cracking.

This is supported further by the facts that (1) three is the smallest number of cracks for which a kinematically possible failure mechanism is created (fig. 7), (2) the number of cracks is limited to three to five by the large aggregates ( $d_{max} = 8$  mm) and (3) three cracks result in the lowest peak stress and the most brittle post-peak behaviour. Since concrete cracking is not perfectly brittle, a stress-crack-opening relation with linear softening up to  $\delta_u = 0.03$  mm was used in the simulations (Fig. 6b, [4]).

Fig. 8 gives the residual pressure in the arapree as a function of the initial pressure. It shows that failure changes from ductile to brittle when the diameter of the concrete prism increases. Failure takes place due to the growth of the radial cracks from the inside to the outside. The maximum residual pressure is found when the crack front reaches the outside of the prism.

## 6 de Sitter and Vonk

Due to the relatively small size of the prisms, the average opening of the cracks is still small when this happens, which means that the crack stresses have not entered far in the softening branch of fig. 6b and still have a significant value over the total length of the cracks.

The simulations indicate that an elastoplastic model can give good predictions of the maximum allowable initial pressure in the arapree. For  $(d_c/d)^2 \gg 1$  the theory of elasticity yields:

$$p_{r_i} = \left(1 + \frac{E_{res}(1+\nu_c)}{E_c(1-\nu_{res})}\right) p_r$$

with  $d_c = 2r_0 = 2(r_i + c)$

This relation is shown in fig. 8 as the tangent in the origin. According to the theory of plasticity, the maximum residual pressure is:

$$p_r = (d_c - d) f_{ct} / d \quad (5.2)$$

An estimate of the maximum allowable pressure in the arapree is found by calculating the intersection point between the elastic and the plastic line, which gives

$$P_{r_{max}} = 2c \left(1 + \frac{E_{res}(1+\nu_c)}{E_c(1-\nu_{res})}\right) f_{ct} \quad (5.3)$$

The result for  $f_{ct} = 3.4$  MPa,  $E_{res} = 4000$  MPa and  $E_c = 30\,000$  MPa is shown in fig. 8.

According to an energy approach, failure can only take place when the initial elastic deformation energy in the arapree:

$$E_{ea} = \frac{\pi(1-\nu_{res})}{4} \frac{p_{r_i}^2 d^2}{E_{res}} \quad (5.4)$$

is at least equal to the energy needed to create the three radial cracks

$$E_{fc} = 3c G_{fc} \quad (5.5)$$

This results in

$$p_{r_{max}} = \left( \frac{12c E_{res} G_{fc}}{\pi d^2 (1-\nu_{res})} \right)^{\frac{1}{2}} \quad (5.6)$$

The fracture energy  $G_{fc}$  can be determined in tests and is equal to  $0.5 f_{ct} \delta_u$  in the simulations with the computer program UDEC (see fig. 6b)

In a third approach the minimum expansion  $\Delta d$  of the arapree upon relief of the prestress, necessary to find a crack opening  $\delta_u$  for the three cracks, can be calculated. Because the concrete pieces move as rigid blocks, as they are stress-free before and after the relief of the prestress, this calculation results in the simple relation.

$$2\Delta r_i = \Delta d = \frac{\delta_u}{\sqrt{3}} \quad (5.7)$$

According to equation 2 this expansion corresponds to an initial pressure in the arapree:

$$p_{r_{imax}} = \frac{E_{res}}{(1-\nu_{res})} \frac{\delta_u}{d\sqrt{3}} \quad (5.8)$$

The results of the three approaches are compared in fig 9 for  $d = 5.7$  mm. The fact that the curves for the energy approach and the deformation approach give higher allowable pressures for small diameters of the concrete prism than the elastoplastic approach indicates the ductile character of the failure for those diameters. For larger diameter a more brittle failure is predicted by the models. This is all in accordance with the results of the computer simulations. The preferable design curve is that of the elastoplastic approach because it guarantees a residual stress which is close to the maximum. It will result in the highest shear-stress transfer and thus in the shortest transfer length of the prestress in the anchorage zone. Attention should be given to the required safety factor as the failure of the concrete prisms is brittle for large diameters and a delayed crack growth is observed in the tests of section 4.

Fig. 9 gives also a comparison of the model predictions and the test results of section 4. It shows that the test results agree with the elastoplastic model. The deformation approach is found to be very conservative. One additional comparison with test results can be made. Concrete prisms with a square cross-section of  $25 \times 25$  mm<sup>2</sup> made of a special high-strength Densit mortar ( $f_{ct} = 11$  MPa,  $f_{cc} = 180$  MPa,  $E_c = 65000$  MPa) were also pretensioned with a force of 17 kN ( $p_i = 27.5$  MPa). The elastoplastic model, the energy model and the deformation model predict an allowable initial stress  $p_i$  of 41.5, 33.9 and 18.7 MPa, respectively.

## 8 de Sitter and Vonk

The successful production of the prisms agrees with the first two models. The prisms cracked when they were submerged in water of 60°C. According to the equations in section 2, the rise in temperature increased the initial pressure in the arapree to 42.3 MPa, which is more than the elastoplastic model and the energy model allow.

### Conclusions

Three approaches to calculate the critical initial confined radial pressure  $p_{r,max}$  have been presented; the deformation criterium, the elasto plastic criterium and the fracture energy criterium. Based on a very limited number of tests and practical experience the following preliminary conclusions are drawn.

- 1) In FRPR pretensioned concrete the confined radial deformations (Hoyer effect) are critical for splitting forces.
- 2) The critical confined pressure can be calculated using the elasto plastic criterium (5.3)
- 3) A safer value for  $p_{r,max}$  may be obtained by comparison of the elasto plastic criterium and the fracture energy criterium (5.6) and taking the smallest value.
- 4) Due to interaction with the Hoyer effect there is a significant difference between bond in push-in tests and bond in pull-out tests. Hence transfer lengths should either be directly measured or based on measurements of bond in push-in tests.

### NEW DEVELOPMENTS

AKZO and HBG have developed a compressible coating for FRPR (as well as epoxy coated strands) in order to reduce radial stresses due to the Hoyer effect and incompatible temperature expansion coefficients. Short duration tests have shown that this coating solves the problem. There is an influence on bond but transfer lengths remain significantly less than for steel strands. Long duration tests are in progress. If these tests are successful a major obstacle to the use of FRPR in thin pretensioned concrete elements will have been removed. A patent application has been submitted.

### REFERENCES

- [1] Sarneel, R.G.M.; 1 "Het aanhechtingsgedrag van Arapree aan lichtbeton" deel 1 & 2 ( in Dutch) MSc. report may 1990 Eindhoven University of Technology.
- [2] Gils, A.W.M. van; "Overdrachtslengte en het optreden van spijtscheuren bij Arapree  $\phi$  5 mm" deel 1 & 2 (in Dutch) MSc. report july 1991 Eindhoven University of Technology.

[3] Egas, M.; Sitter, W.R. de; "Tests on Arapree Pretensioned Sleepers" International Symposium on precast Railway Sleepers; Madrid april 1991 Monograficos 8. Collegio de Ingenieros de Caminos, Canales y Puertos

[4] Vonk, R.A.; "Softening of Concrete loaded in Compression" Ph.D. Thesis june 1992 Eindhoven University of Technology.

### SYMBOLS

c	cover ; mm
d	bar diameter ; mm
$d_c$	concrete cylinder diameter ; mm
$f_{ct}$	tensile spl.strength; MPa
p	pressure; MPa
$r_1$	radius of bar; mm
$r_0$	outer radius of cylinder; mm
A	area ; mm <sup>2</sup>
E	Young's moduljus; MPa
$E_{def}$	deformation energy; Nmm/mm
F	force ; N
$G_f$	fracture energy; Nmm/mm
$\alpha$	thermal expansion; 1/°C
$\delta$	crack opening ; mm
$\varepsilon$	strain
$\phi$	angle
$\nu$	Poisson coefficient
$\tau$	shear stress; MPa
$\sigma$	normal stress; MPa
$\Delta T$	temp. difference ; °C
$\Delta r_i$	radial expansion; mm

### indices:

c	concrete
f	fiber
res	resin
r	radial direction
l	longitudinal
t	tangential
i	initial

TABLE 1 — BOND IN PULL-OUT/PUSH-IN CONDITIONS

series	Pull-out					Push-in				
	1	2	3	4	5	1	2	3	4	
cover	21	28	35	35	35	21	28	35	35	mm
cracks	yes	no	no	no	no	yes	yes	no	yes	
$T_{max}$	8.4	4.77	6.74	7.89	7.20	6.89	6.25	11.07	8.78	MPa
$f_{ct}$	2.35	2.37	1.61	2.41	2.30	2.10	2.45	1.61	2.41	MPa
$F_1$	3.94	2.47	5.85	6.59	0	20.4	20.18	13.9	18.1	kN
$F_2$	11.33	6.67	11.78	13.53	6.34	26.64	25.68	23.64	2582	kN

TABLE 2 — OCCURRENCE OF CRACKING

texture	30 x 30 mm <sup>2</sup>	35 x 35 mm <sup>2</sup>	40 x 40 mm <sup>2</sup>	45x 45 mm <sup>2</sup>
coarse	yes	yes	later	no
normal	yes	yes	later	no
fine	yes	yes	no	no
smooth	yes	yes	later	no

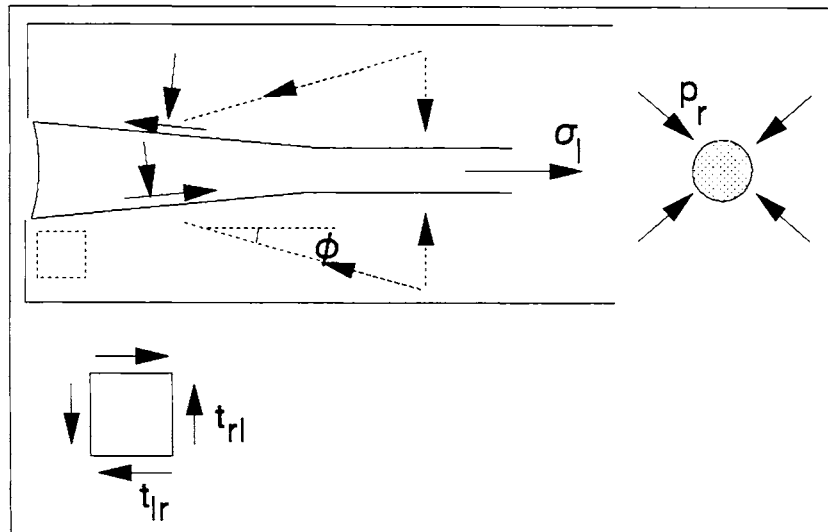


Fig. 1—Hoyer effect